Analytical Sciences
https://doi.org/10.1007/s44211-025-00755-3

ORIGINAL PAPER

Ultra-sensitive biosensor detection of microRNA based on the CRISPR/Cas12a system and exonuclease-assisted target recycling signal amplification

Xing Yang[1] · Yu Luo[1] · Chunhua Su[3] · Zhimei Huang[1] · Yafang Tang[1] · Liwen Zhang[2]

Received: 3 November 2024 / Accepted: 20 March 2025
© The Author(s), under exclusive licence to The Japan Society for Analytical Chemistry 2025

Abstract

MicroRNAs (miRNAs) are essential regulators of gene expression and are significantly involved in both preventing and treating a range of diseases. To that end, we developed an ultra-sensitive detection method for miRNA-141 by integrating exonuclease-assisted target recycling signal amplification with the CRISPR/Cas12a system. This method employs a variable hairpin probe (HP) designed to hybridize with miRNA, which, under the action of exonuclease III (ExoIII), cleaves the hairpin probe and triggers target recycling signal amplification. This results in the formation of output DNAs (ODs) containing multiple repeat sequences. The CRISPR/Cas12a system identifies these repeated sequences in ODs through its crRNA component, which in turn triggers the trans-cleavage function of the Cas12a/crRNA complex. It leads to the cleavage of a fluorescently quenched reporter probe. Consequently, this process restores fluorescence, producing a significantly enhanced fluorescent signal that facilitates the detection of miRNA-141, achieving a detection threshold down to 62 fM. This detection approach can specifically differentiate miRNA-141 from other confounding substances and has effectively identified low concentrations of miRNA-141 in actual sample human serum and diverse cancer cell lysates, showcasing its capability for tracing various nucleic acid biomarkers at minimal levels.

Keywords CRISPR/Cas12a · MiRNA-141 · ExoIII · Target recycling signal amplification

Introduction

Clustered regularly interspaced short palindromic repeats (CRISPR) and associated Cas nuclease proteins are extensively utilized across various scientific disciplines [1, 2]. The derived RNAs (crRNA, sgRNA) produced from CRISPR transcription and processing assembles with Cas proteins to form the CRISPR/Cas complex, which is capable of recognizing and cleaving invading nucleic acids. The crRNA and sgRNA are programmable, allowing them to recognize and bind to a wide range of target nucleic acids. This activates the cutting activity of Cas enzymes, making them highly versatile [3]. Currently, diagnostic systems based on Cas9 [4, 5], Cas12a [6, 7], Cas13a [8], and Cas14a [9] have been established to detect various target molecules. The revolutionary CRISPR/Cas system has not only played a significant role in gene editing [10, 11], but also demonstrates significant promise in developing biosensors for detecting nucleic acids and small molecules, attributed to its high precision and user-friendliness [12–14]. Cas12a, a single RNA-guided protease, exhibits both cis-cleavage and trans-cleavage capabilities. Its trans-cleavage activity refers to the nonspecific cleavage of surrounding ssDNA after the crRNA binds to dsDNA or ssDNA. Guided by crRNA, Cas12a can recognize dsDNA targets that contain a short T-rich PAM (5′-TTTN-3′) sequence [15, 16]. The outstanding sensitivity and specificity of Cas12a significantly enhance the diversity of sensor designs based on this system. CRISPR/

✉ Yafang Tang
tangavonrs@163.com

✉ Liwen Zhang
zlw@glmc.edu.cn

1 Clinical Research Center for Neurological Diseases of Guangxi Province, Affiliated Hospital of Guilin Medical University, Guilin 541004, China

2 Information Center, Guilin Medical University, Guilin 541199, Guangxi, China

3 Department of Cardiovascular Medicine, Second Affiliated Hospital of Guilin Medical University, Guilin 541100, China

Published online: 21 April 2025

Cas12a has demonstrated significant promise in detecting tumor biomarkers.

MiRNAs are important endogenous non-coding small RNA molecules, typically composed of 21–25 nucleotides [17]. As a novel class of biomarkers, miRNAs are closely associated with the occurrence and development of diseases such as cancer [18, 19]. Compared to other RNA types, miRNAs exhibit better chemical stability, making them significant biological markers for early cancer diagnosis and treatment prognosis [20, 21]. Therefore, achieving rapid and accurate detection of miRNAs holds considerable clinical significance. However, in practical detection, the low expression abundance and short sequences of miRNAs pose challenges. Existing detection methods often suffer from long reaction times and susceptibility to interference from complex biological environments, making the rapid and ultrasensitive detection of miRNAs a great challenge.

MiRNA-141, a small regulatory molecule, is key in regulating specific miRNA activities, influencing cell proliferation, differentiation, and apoptosis [22–25]. Abnormal expression of miRNA-141 has been found in prostate cancer [26], lung cancer [27], liver cancer [28], and gastric cancer [29, 30], highlighting its potential as an important biomarker for early cancer monitoring. However, due to its inherent sensitivity, low abundance, and high sequence homology, achieving high sensitivity and selectivity in the detection of miRNA-141 is particularly challenging. Thus, establishing an accurate method for monitoring miRNA-141 is vital for cancer diagnosis and prognosis. In recent years, fluorescence analysis methods based on nanomaterials have been recognized as powerful tools for detecting microRNAs due to their high sensitivity [31].

For instance, Liu et al. [32] designed a gold nanoparticle (AuNPs)-based target-triggered catalytic hairpin assembly (CHA) for detecting miRNA-21. Zhang et al. [33] developed an AuNPs-based DNA walker for the analysis of bladder cancer-related exosomal miR-133b and miR-135b. Although these sensing methods exhibit excellent analytical performance, the requirement for preparing nanomaterials may increase the complexity of the analysis. Zhou et al. [34] constructed a simple yet versatile Exo III powered cascade DNAzyme amplifier with an ultralow background for highly sensitive and selective microRNA assay in vitro and even in living cells. Wang et al. [35] propose a novel Exo III-propelled DNAzyme cascade for sensitive and highly efficient miRNA analysis. However, the activity of most DNAzymes depends on specific metal ions [36]. DNAzymes may nonspecifically interact with other nucleic acids, leading to unintended gene silencing or other biological effects [37]. CRISPR-Cas12a can effectively identify the presence of specific nucleic acid targets and small changes in sequences, which is particularly important for nucleic acid identification [38]. Chen et al. [39] Using miRNA targets as spacer RNA and another single-stranded DNA as the activator, split Cas12a system-based fluorescence and rapid lateral flow assays were developed with specificity and novelty. However, they lack target signal amplification. This study employed the CRISPR/Cas12a system and exonuclease-assisted target recycling signal amplification methods for miRNA detection analysis, enhancing sensitivity and accuracy.

Hence, we designed a detection method for miRNA-141 based on the CRISPR/Cas12a system and an exonuclease-assisted target recycling signal amplification strategy. This method involves constructing an HP complementary to the target miRNA-141. Upon the presence of the target, the HP attaches to the target miRNA, creating a blunt-ended hairpin structure. Exo III then cleaves the HP from the 3' blunt end, releasing the target and allowing for further reactions, thereby enabling cyclic signal amplification. Subsequently, a large amount of ODs is generated. These multiple repeat sequences of ODs can bind to and activate the trans-cleavage activity of Cas12a/crRNA, leading to the cleavage of a fluorescently quenched reporter probe, leading to a significantly enhanced fluorescent signal for ultra-sensitive detection of miRNA-141. Furthermore, this method successfully detects low levels of miRNA-141 in actual sample human serum and various cancer cell lysates.

Experimental

Reagents and materials

Gel-Red nucleic acid dye was purchased from Biyutian Biotechnology Co., Ltd. Agarose G-10 from Biowest, Spain. ExoIII and Cas12a were obtained from New England Biolabs, USA. Cell culture medium 1640 and Dulbecco's Modified Eagle Medium (DMEM) were purchased from Thermo Fisher Scientific (Suzhou) Instruments Co., Ltd; fetal bovine serum (FBS), trypsin digestion solution, and penicillin–streptomycin were obtained from Sigma, USA; human prostate cancer cells (22Rv1), human cervical squamous cell carcinoma cells (SiHa), human breast cancer cells (MCF-7), and human microglial cells (HMC3) were obtained from the Cell Bank of the Chinese Academy of Sciences (Shanghai, China). 5 × TBE (Tris-Boric acid and EDTA) was purchased from Solarbio Biotechnology Co., Ltd (Beijing, China). Tris–EDTA, the HPLC-purified DNA, and RNA were synthesized by Sangon Biotechnology Co., Ltd (Shanghai, China). The DNA and RNA sequences are listed in Table 1. The index of significant abbreviations is listed in Table S1.

Table 1 Sequence of the used oligonucleotides[a]

Oligonucleotide	Sequences (5′-3′)
miRNA-141	*TAACACTGTCTGGTAAA*GATGG
HP	**CTGTTAGGTAGGTAGA**TAAATGGGAACTCGCGACTCT ACCTACCTAACAG*TTTACCAGACAGTGTTA*
crRNA	UAAUUUCUACUAAGUGUAGAU**UCUACC UACCUAACAG**
reporter probe	FAM-TTATT-BHQ1
1M-1	TAACACTGTCTAGTAAAGATGG
1M-2	TAACACTGTCTGGTAAAGGTGG
2M-1	TAACACTCTCTGGTAGAGATGG
2M-2	TAACACTGTCAGGTAAAGATCG
5M	TAACTCTGTATGGCAATGATGC
7M	GAAGACAGTCTCGTTAACATGC
miRNA-21	TAGCTTATCAGACTGATGTTGA
miRNA-122	TGGAGTGTGACAATGGTGTTTG

[a]The italic part of the base is the specific binding sequence between the hairpin probe and miRNA-141. The HP sequence underlined section is ODs. The bold black part of the base is the binding sequence between ODs and crRNA within the sequences. Underscores indicate mismatched base positions. T bases replaced the U bases of miRNA-141

Solution preparation

DNA stock solution: first, put the DNA powder centrifuge at 5000 rpm for 5 min. After centrifugation, add Tris–EDTA to the DNA centrifuge tube to dissolve it, forming a final concentration of 100 μM DNA stock solution. Denature the HP chain at 95 °C for 5 min, cool to room temperature to obtain stable hairpin probes. Divide the stock solution and denatured hairpin probes into centrifuge tubes, and store them in a − 20 °C freezer for later use.

MiRNA detection procedures

Initially, Cas12a (50 nM) and crRNA (150 nM) were combined in 1 × NEBuffer™ 2.1 buffer and allowed to incubate at 37 °C for 15 min to obtain the Cas12a/crRNA complex. The sensing analysis for miRNA-141 consists of two main processes: exonuclease-assisted target recycling signal amplification and the recognition and cleavage by the CRISPR/Cas12a system. Exonuclease-assisted target recycling reaction: in a reaction tube, 5.0 μL of HP (2 μM), 10.0 μL of different concentrations of miRNA, 8.0 μL of Exo III (1 U/μL), 4.0 μL of NE Buffer 1, and 13.0 μL of ddH_2O were combined and incubated in a 37 °C water bath for 80 min. Recognition and Cleavage by the CRISPR/Cas12a System: the enzyme-cleaved reaction mixture, along with 6.0 μL of Cas12a/crRNA, 5.0 μL of the reporter probe (2 μM), and 6.0 μL of NE Buffer 1, were incubated at 37 °C for 60 min. Finally, the mixture was diluted with ddH_2O to a total volume of 100 μL for fluorescence measurement. The fixed excitation wavelength is 490 nm, and the emission spectrum in the range of 515–620 nm (slit = 5 nm) is collected with the RF-7000 Hitachi spectrophotometer.

Agarose gel electrophoresis experiment

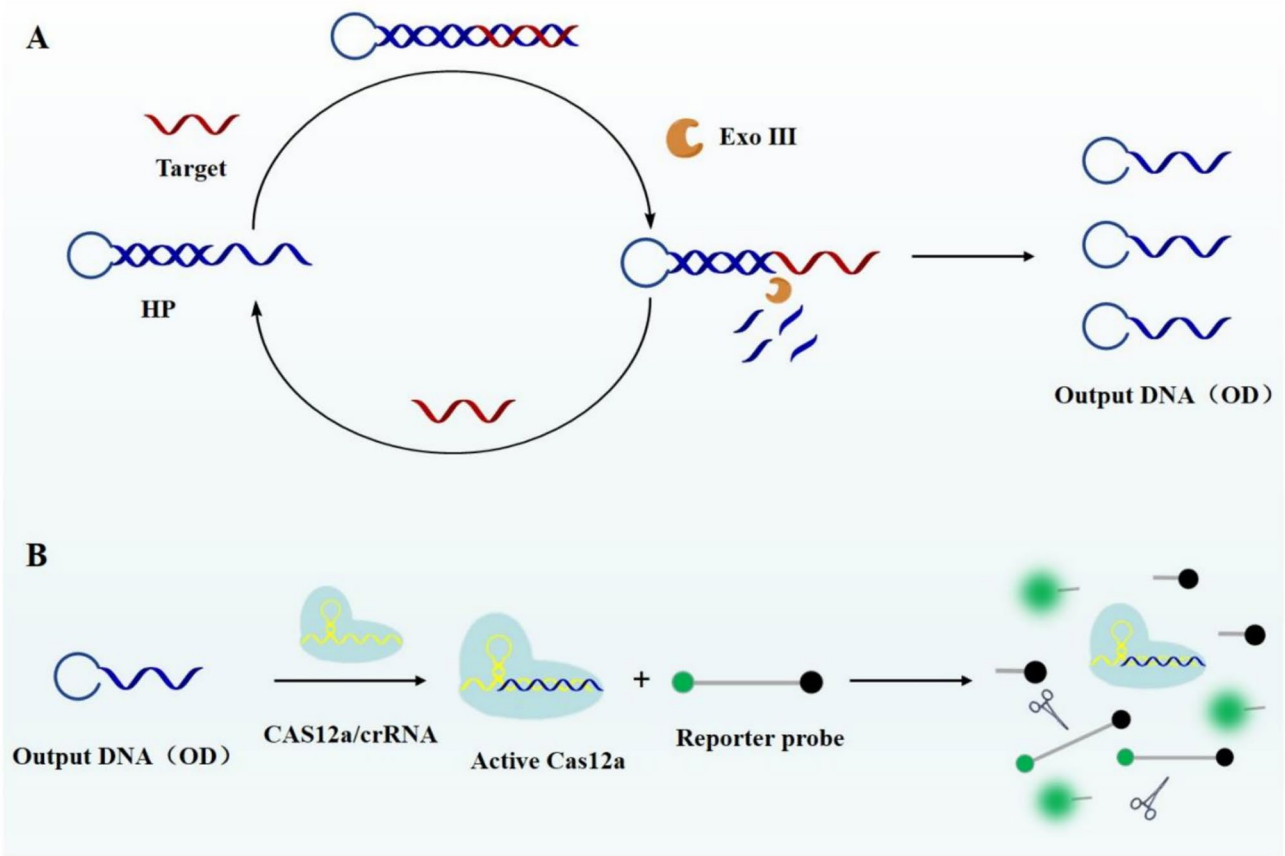
First, 2.5 g agarose G-10 was weighed into a conical bottle, then 100 mL of the prepared 0.5 × TBE solution was added, microwave oven was heated for 3 min, and 10 μL gel red nucleic acid dye was added, shake well, and poured into the glue making mold for 30 min to make 2.5% agarose gel. Secondly, 0.5 × TBE buffer was added to the electrophoresis tank, and 10 μL final reaction solution was added to each sample adding hole, and electrophoresis separated for 60 min at a voltage of 100 V. Finally, the agarose gel was placed under the AlphaImager HP gel imaging system to observe the electrophoretic results, and the photo-analysis was performed according to the size of the exposure.

Serum sample analysis

For the assay of miRNA-141 in human serum, the targets of 0.4, 5.0, 5.0×10^2, and 1.0×10^3 pM were added to 1% of the human serum sample, and the other experimental steps were the same as miRNA detection procedures. The calculation method for Found (pM) is to subtract the serum blank's fluorescence value from the spiked serum's fluorescence value and then substitute it into the linear equation. Recovery (%) = Found (pM)/Added (pM) × 100%.

Cell culture and cell lysate preparation

22Rv1, SiHa, and HMC3 cells were grown in RPMI1640 medium, and MCF-7 cells' culture medium was DMEM medium with 10% FBS and 100 U/mL of penicillin and streptomycin. Cells were cultured at 37 °C in a cell incubator with 5% CO_2, respectively. The actual samples used in



Scheme 1 Schematic illustration of (**A**) exonuclease-assisted target recycling signal amplification. (**B**) Activation process of CRISPR/Cas12a system

the analysis of complex samples in this experiment are cell lysates of various cell lines. The cell suspension was centrifuged at 4 °C with 1000 r/min for 5 min, removed the culture medium, washed it once with PBS buffer, and then added 1 mL PBS buffer to resuspension the cells. Cells density were determined by counting with the Denovix CellDrop BF cell counter. The cells were centrifuged at 4 °C with 1000 r/min for 5 min, removed the PBS buffer, and then added 200 µL PBS buffer to resuspension the cells. Then, the cells were crushed by ultrasonic for 15 min in the ice water bath. After breaking, the cell homogenate was centrifuged at 4 °C with 12,000 r/min for 20 min. The supernatant was taken as the cell lysate sample and stored at − 20 °C for reserve.

Results and discussion

The detection principle of microRNA sensing method

The method for sensitive detection of miRNA-141, which relies on enzymatic cleavage of target recycling reactions and subsequent recognition and cleavage by the CRISPR/Cas12a system, is depicted in Scheme 1. Scheme 1A is the enzymatic cleavage of target recycling reactions. The design of the HP features a 3′ protruding to prevent degradation by Exo III while allowing recognition by the target miRNA-141. When the target is present, the HP binds to the target miRNA, forming a 3′ blunt end HP/miRNA-141 hybridization complex. Exo III specifically cleaves the HP/miRNA-141 hybridization complex in the 3′ to 5′ direction, progressively removing single nucleotides and releasing the target. The released target continues the reaction, enabling cyclic signal amplification. Following Exo III cleavage, a ODs containing multiple repeat sequences is formed. Scheme 1B, ODs is recognized by the crRNA of the CRISPR/Cas12a system, activating the trans-cleavage activity of Cas12a/crRNA. This results in the cleavage of the fluorescently quenched reporter probe, restoring fluorescence and generating a sharply amplified fluorescent signal for the ultra-sensitive detection of miRNA-141. Conversely, when the target is absent, the 3' protruding of the HP cannot be cleaved by Exo III, preventing the formation of ODs with repeat sequences. Consequently, the trans-cleavage activity of the CRISPR/

Cas12a system is not activated, and the quenched reporter probe only displays very low fluorescence.

Feasibility experiment

Initially, the feasibility of this method for microRNA detection was further validated by measuring the fluorescence intensity. As shown in Fig. 1, the reporter probe is modified with a FAM fluorescent group on one side and a BHQ1 quenching group on the other, resulting in fluorescence quenching of the reporter probe. When the target is absent, the fluorescence emission intensity of the mixture containing HP + reporter probe + Exo III + Cas12a/crRNA is very weak, indicating that Cas12a remains in an inactive state. When a target concentration of 10 pM is added to this mixture, it triggers the enzyme-cleaved circular reaction, producing multiple repeat sequences of ODs, which in turn activate the trans-cleavage activity of Cas12a. This results in the cleavage of the quenched reporter probe and an enhancement of the fluorescence signal, demonstrating a significant difference in fluorescence. Furthermore, when the target concentration is increased to 1 nM, the fluorescence signal is stronger compared to that at 10 pM, confirming the feasibility of the method.

Additionally, to further validate the exonuclease-assisted target recycling reaction and the recognition and cleavage by the CRISPR/Cas12a system, agarose gel electrophoresis experiments were conducted, and the results are shown in Fig. 2. Lane 1 is the band of the HP strand, and the position of the lane 2 band does not change after adding Exo III,

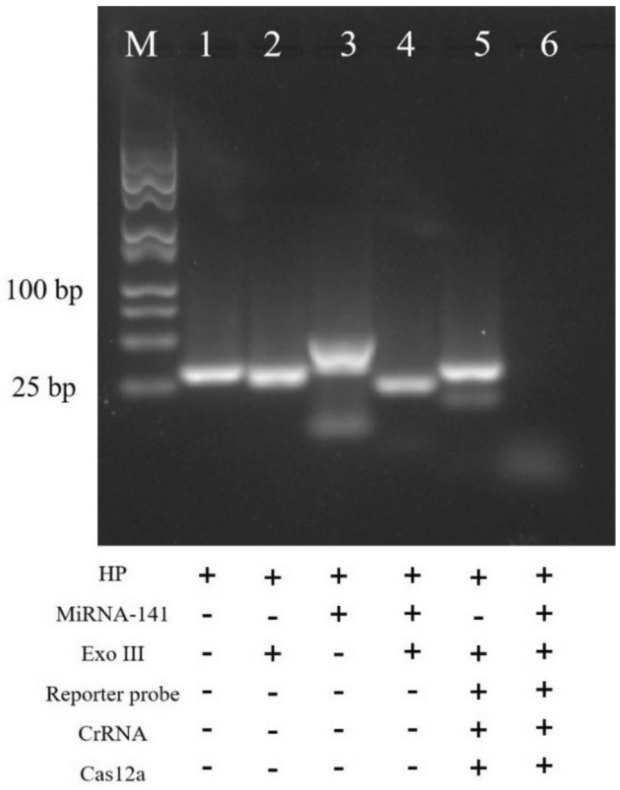


Fig. 2 Gel electrophoresis analysis. Lane M: DNA marker; lane 1: HP; lane 2: HP + ExoIII; lane 3: HP + miRNA-141; lane 4: HP + miRNA-141 + ExoIII; lane 5: HP + reporter probe + ExoIII + Cas12a + crRNA; lane 6: miRNA-141 + HP + reporter probe + ExoIII + Cas12a + crRNA

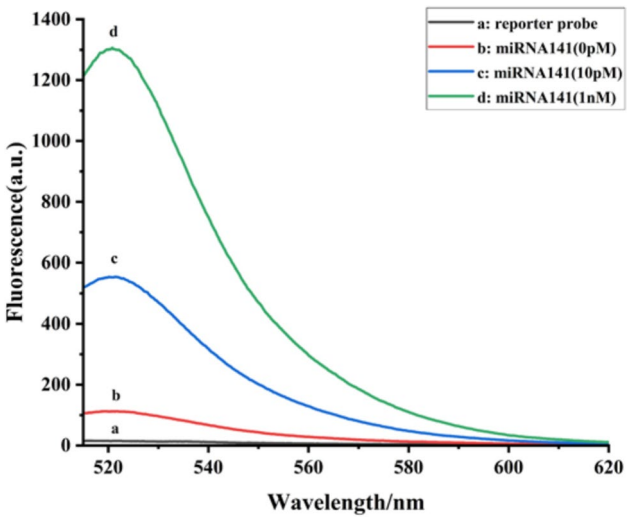


Fig. 1 Fluorescence analysis of different treatments: curve (a) reporter probe; curve (b) miRNA141 (0 pM) + HP + reporter probe + Cas12a/crRNA + ExoIII; curve (c) miRNA141 (10 pM) + HP + reporter probe + ExoIII + Cas12a/crRNA; curve (d) miRNA141 (1 nM) + HP + reporter probe + ExoIII + Cas12a/crRNA

indicating that the 3′ protruding end of HP can resist enzyme degradation. When added with miRNA-141 but without ExoIII, a large bright band appeared in the high base region in lane 3. In lane 3, the band appears at a higher base weight than in lane 1, suggesting that the target is bound to the hairpin probe, forming an HP/miRNA-141 hybridization complex. Lane 3 has a band below 25 bp, the miRNA-141 band. Then, the large band disappeared after Exo III was added to lane 4, which indicates that the HP/miRNA-141 double strand was digested by Exo III, resulting in a slightly lower base number of strands. The HP/miRNA-141 double strand was digested by Exo III to form a new bright band that was the ODs strand. In lane 4, bands below 25 bp are fragments of miRNA-141 produced by enzymatic digestion. In lane 5, the two bands are HP and crRNA. However, after adding miRNA-141 in lane 6, the HP band and crRNA band disappeared compared with lane 5, indicating that HP and target combined to form HP/miRNA-141 hybrid complex. Exo III degrades the complex and releases the target. ODs bind with Cas12/crRNA to form an active enzyme, the reporter probe is recognized and cut by the CRISPR/Cas12a system, leaving the fragments produced after enzymatic digestion.

Therefore, it is verified that the strategy of hybridization and enzyme digestion of DNA is viable.

Optimization of experimental parameters

To ensure optimal sensing performance of the method, we investigated various factors, including the concentration of Exo III, reaction time for Exo III, concentration of Cas12a/crRNA, and enzyme reaction time for Cas12a/crRNA. The concentration of microRNA-141 is 1 nM. As depicted in Fig. S1A, the fluorescence intensity notably rose with higher concentrations of Exo III in the range of 2–10 U/μL, reaching a plateau at 8 U/μL. Thus, the optimal concentration of the enzyme was determined to be 8 U/μL. We also explored the impact of Exo III reaction time on the yield of ODs. As illustrated in Fig. S1B, as the reaction time for Exo III was extended from 20 to 100 min, the fluorescence intensity continually increased, stabilizing afterward. Therefore, we selected 80 min as the optimal reaction time for Exo III. The amount of Cas12a/crRNA enzyme determines the efficiency of its trans-cleavage activity, so we further examined the effect of Cas12a/crRNA concentration on fluorescence signal intensity. Figure S1C shows that as the concentration of Cas12a/crRNA increased from 1 to 3 nM, the fluorescence intensity continued to rise. However, further increases in Cas12a/crRNA concentration did not result in additional enhancement of the fluorescence signal, indicating that an appropriate increase in Cas12a/crRNA concentration helps achieve optimal fluorescence intensity while conserving enzyme usage. Next, we investigated the cutting time of Cas12a/crRNA. As illustrated in Fig. S1D, the fluorescence intensity increased with prolonged cutting time up to 60 min, after which no significant changes were observed. Thus, 60 min was chosen as the optimal cutting time. In summary, the optimal parameters determined were: Exo III concentration of 8 U/μL, Exo III reaction time of 80 min, Cas12a/crRNA concentration of 3 nM, and Cas12a/crRNA cutting time of 60 min.

Sensitivity analysis of miRNA detection

After establishing the optimal experimental parameters, we examined the change in fluorescence intensity with varying concentrations of miRNA-141 and evaluated the analytical performance of the amplification strategy for detecting miRNA-141. Figure 3A displays the characteristic emission spectra corresponding to different target concentrations. The results indicate that as the target concentration increased from 0 pM to 10 nM, the fluorescence intensity consistently rose. Figure 3B displays the linear equation is $Y = 279.7139X + 242.7505$ ($Y = F - F_0$, $X = \log_{10} c$) and the linear correlation coefficient is $R^2 = 0.995$. We observed a linear relationship between fluorescence intensity and the logarithm of miRNA-141 concentration. Finally, using this fitting equation and the 3σ method, we determined the detection limit to be 62 fM. Compared to previously reported CRISPR/Cas12a detection methods (Table S2), our designed sensing method demonstrates significantly enhanced sensitivity for detecting microRNAs.

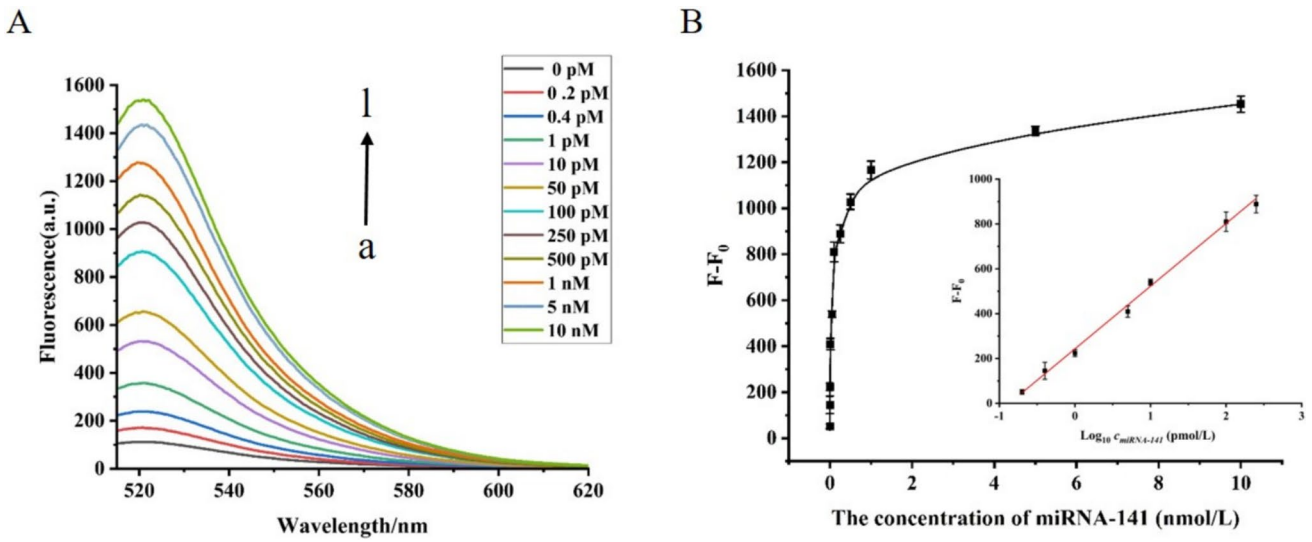


Fig. 3 **A** Fluorescence spectra corresponding to 0, 200 fM, 400 fM, 1 pM, 10 pM, 50 pM, 100 pM, 250 pM, 500 pM, 1 nM, 5 nM, and10 nM of target miRNA-141 (from a to l) detected by the method. **B** The curve of the relationship between targets concentration and ($F - F_0$). The illustration shows the standard curve and linear equation for detection of miRNA-141. The data were expressed as mean ± SD (n = 3)

Specificity analysis

To investigate the specificity of this method for detecting miRNA-141, we selected miRNA-21, miRNA-122, and base-mismatched sequences as interference sequences. Among these, miRNA-21 and miRNA-122 served as random control sequences, while the 1M-1, 1M-2, 2M-1, 2M-2, 5M, and 7M mismatched sequences contained mutated bases in the domain of miRNA-141. As shown in Fig. 4, the fluorescence signals of miRNA-21, miRNA-122, and base mismatch sequences are much weaker than those of samples containing target miRNA-141. Additionally, the mixtures of miRNA-141 and other controls displayed fluorescence intensities similar to the target miRNA-141. This indicates that the sensing method maintains strong specificity for miRNA-141 even in high concentrations of interference sequences.

Actual sample analysis

Finally, we discussed the practical application of CRISPR/Cas12a system and exonuclease-assisted target recycling signal amplification in biological environment. Figure 5 shows the fluorescence spectra of miRNA-141 analyzed in serum free and serum samples. Although the fluorescence intensity of the system in serum is biased, there was no significant interference with the analysis of the target. The experiment tested the serum with different targets concentrations (Table S3). The recovery range was 97.50–115.40% with RSD of 3.45–9.51% for three parallel tests. There was no obvious interference in the analysis of targets, demonstrating the biosensor method's high accuracy in complex biological samples.

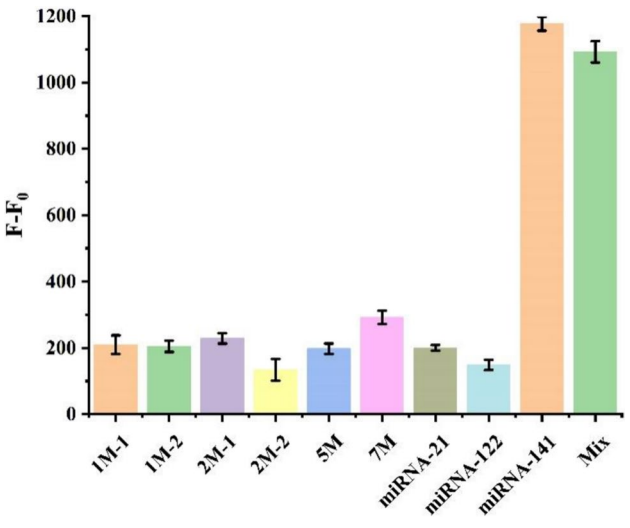


Fig. 4 Selectivity investigation of the microRNA-141 sensing system. The concentrations of microRNA-21, microRNA-122, and the base-mismatched sequences were all 1 nM

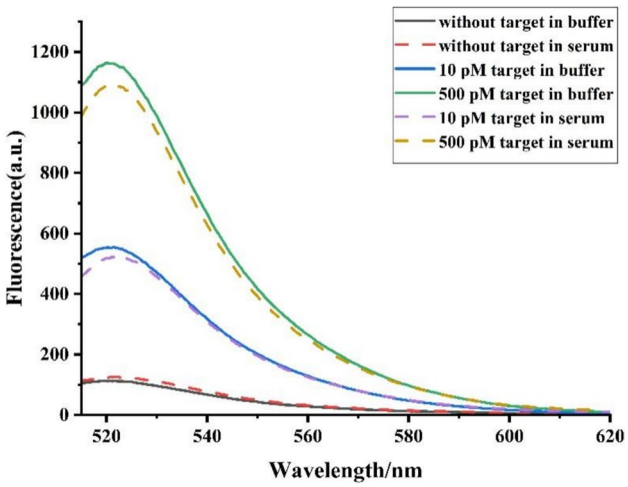


Fig. 5 Exonuclease-assisted target recycling signal amplification biosensor in buffer and serum samples

To confirm the method's applicability to real samples, we assessed miRNA-141 levels in 1000 cells μL^{-1} diverse cancer cell lysates, including 22Rv1, MCF-7, SiHa, and HMC3. As shown in Fig. S2, the fluorescence signal from the HMC3 cell lysate incubated samples showed only a slight increase compared to the blank control. In contrast, the expression of miRNA-141 gradually increased in SiHa, MCF-7, and 22Rv1 cells. Notably, miRNA-141 was overexpressed in 22Rv1 cells, resulting in the highest fluorescence intensity observed in the sample solution analyzed by fluorescence spectrophotometry [40]. Figure 6A presents a bar graph of fluorescence intensity increases with the number of miRNA-141 cells in the range of 10 to 10^5 cells μL^{-1}. Figure 6B shows a linear plot of fluorescence intensity from different quantities of cell lysates, demonstrating a logarithmic linear correlation between normalized fluorescence intensity and the number of 22Rv1 cells, consistent with previously reported findings [41, 42]. The linear equation is $Y = 266.1252X - 153.8612$ ($Y = F - F_0$, $X = \log_{10} N$, $R^2 = 0.9674$). The results shown here demonstrate that the developed method has the potential for estimating the microRNA expression in cells with good reliability and for providing comprehensive and dependable information for early diagnosis of microRNA-related cancers.

Conclusions

In summary, we have developed a method for detecting microRNA in cancer cell lysates utilizing the CRISPR/Cas12a system and exonuclease-assisted target recycling signal amplification. In our design, Exo III cleavage triggers a cyclic signal amplification reaction, resulting in the formation of ODs containing multiple repeat sequences. These

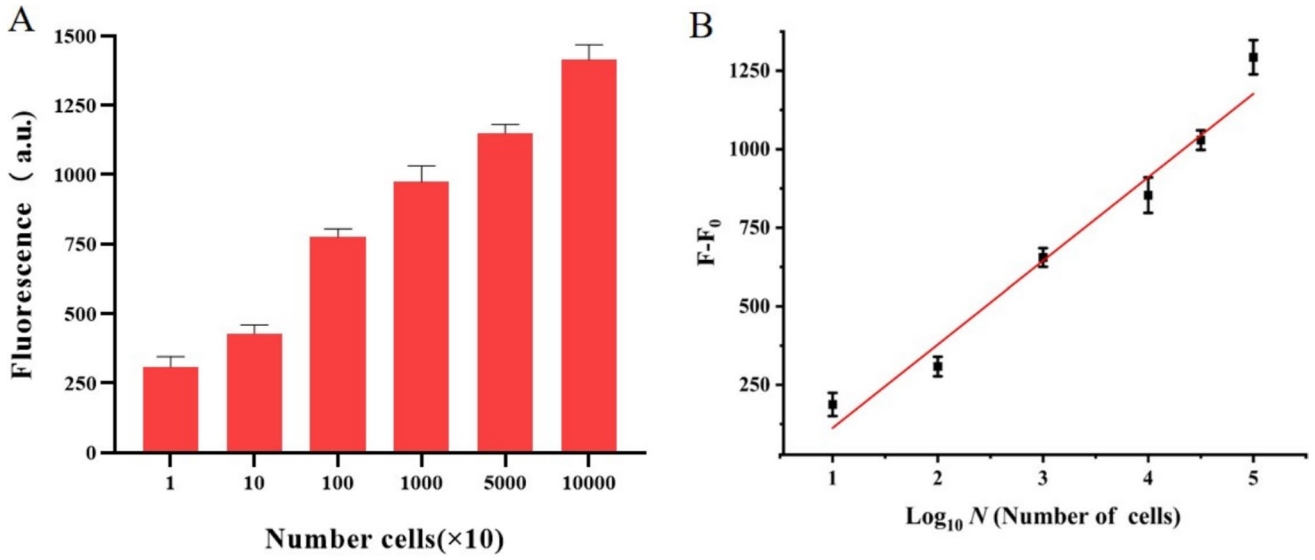


Fig. 6 **A** Histogram of fluorescence intensity of different quantities of cell lysates. **B** Linear graph of fluorescence intensity produced by different amounts of cell lysate. The data were expressed as mean ± SD (n = 3)

repeat sequences can activate the trans-cleavage activity of CRISPR/Cas12a, resulting in the cleavage of the reporter probe and restoring its quenched fluorescence, allowing for highly sensitive analysis of miRNA-141 in human prostate cancer cells. By integrating the signal amplification capabilities of a dual amplification strategy, the detection limit for miRNA-141 is as low as 62 fM. Furthermore, this method has been validated for use in actual sample human serum, various real cancer cell lysates and selective analyses, indicating its potential as a universal tool for detecting trace levels of DNA or RNA biomarkers in biomedical and biological applications. This fluorescence biosensing method shows promising application potential.

Supplementary Information The online version contains supplementary material available at https://doi.org/10.1007/s44211-025-00755-3.

Acknowledgements This work was funded by the Natural Science Foundation of Guangxi Province (Grant No. 2021GXNSFBA 076001), The Basic Ability Enhancement Program for Young and Middle-Aged Teachers in Guangxi Universities (2022KY0491), and Autonomous Region Health Commission Self-funded Research Project (Z-C20240897).

Funding This article is funded by Natural Science Foundation of Guangxi Zhuang Autonomous Region, 2021GXNSFBA 076001, Xing Yang, Middle-aged and Young Teachers' Basic Ability Promotion Project of Guangxi, 2022KY0491, Liwen Zhag, Autonomous region health commission self-funded research project, Z-C20240897, Yu Luo.

Data availability The authors confirm that the data supporting the findings of this study are available within the article.

Declarations

Conflict of interest The authors declare no competing interests.

References

1. E.S. Lander, The heroes of CRISPR. Cell **164**(1–2), 18–28 (2016). https://doi.org/10.1016/j.cell.2015.12.041
2. M. Wang, R. Zhang, J. Li, CRISPR/cas systems redefine nucleic acid detection: principles and methods. Biosens. Bioelectron. **165**, 112430 (2020). https://doi.org/10.1016/j.bios.2020.112430
3. J. Liu, S. Srinivasan, C.Y. Li, I.L. Ho, J. Rose, M. Shaheen et al., Pooled library screening with multiplexed Cpf1 library. Nat. Commun. **10**(1), 3144 (2019). https://doi.org/10.1038/s41467-019-10963-x
4. F. Wang, Y. Hao, Q. Li, J. Li, H. Zhang, X. Zhang et al., Programming PAM antennae for efficient CRISPR-Cas9 DNA editing. Sci. Adv. **6**(19), eaay9948 (2020). https://doi.org/10.1126/sciadv.aay9948
5. R. Zhu, H. Jiang, C. Li, Y. Li, M. Peng, J. Wang et al., CRISPR/Cas9-based point-of-care lateral flow biosensor with improved performance for rapid and robust detection of Mycoplasma pneumonia. Anal. Chim. Acta **1257**, 341175 (2023). https://doi.org/10.1016/j.aca.2023.341175
6. S.Y. Li, Q.X. Cheng, J.K. Liu, X.Q. Nie, G.P. Zhao, J. Wang, CRISPR-Cas12a has both cis- and trans-cleavage activities on single-stranded DNA. Cell Res. **28**(4), 491–493 (2018). https://doi.org/10.1038/s41422-018-0022-x
7. M. Cao, X. Bian, Z. Ji, M. Sohail, F. Zhang, R.J. Linhardt et al., Heparin specifically inhibits CRISPR/Cas12 activation, enabling ultrasensitive heparin detection and gene editing regulation. Anal. Chem. **96**(9), 3970–3978 (2024). https://doi.org/10.1021/acs.analchem.4c00403
8. Y. Shan, X. Zhou, R. Huang, D. Xing, High-fidelity and rapid quantification of miRNA combining crRNA programmability and CRISPR/Cas13a trans-cleavage activity. Anal. Chem. **91**(8), 5278–5285 (2019). https://doi.org/10.1021/acs.analchem.9b00073
9. B. Zhou, R. Yang, M. Sohail, X. Kong, X. Zhang, N. Fu et al., CRISPR/Cas14 provides a promising platform in facile and versatile aptasensing with improved sensitivity. Talanta **254**, 124120 (2023). https://doi.org/10.1016/j.talanta.2022.124120

10. A. Bonini, N. Poma, F. Vivaldi, A. Kirchhain, P. Salvo, D. Bottai et al., Advances in biosensing: the CRISPR/Cas system as a new powerful tool for the detection of nucleic acids. J. Pharm. Biomed. Anal. **192**, 113645 (2021). https://doi.org/10.1016/j.jpba.2020.113645
11. Y. Li, F. Deng, E.M. Goldys, A simple and versatile CRISPR/Cas12a-based immunosensing platform: towards attomolar level sensitivity for small protein diagnostics. Talanta **246**, 123469 (2022). https://doi.org/10.1016/j.talanta.2022.123469
12. S. Peng, Z. Tan, S. Chen, C. Lei, Z. Nie, Integrating CRISPR-Cas12a with a DNA circuit as a generic sensing platform for amplified detection of microRNA. Chem. Sci. **11**(28), 7362–7368 (2020). https://doi.org/10.1039/d0sc03084h
13. L. Dawei, L. Shen, W. Hongsong, Y. Zhaoqi, L. Bei, CRISPR/Cas12a-based biosensors for ultrasensitive tobramycin detection with single and double-stranded DNA activators. Sens. Actuators: B Chem. **355**(355), 131329 (2022). https://doi.org/10.1016/j.snb.2021.131329
14. M. Xiaomei, L. Jinshen, X. Shixiu, X. Jiayao, H. Yong, Z. Shulin et al., Peroxidase-mimicking DNA-Ag/Pt nanoclusters mediated visual biosensor for CEA detection based on rolling circle amplification and CRISPR/Cas 12a. Sens. Actuators: B Chem. **375**(375), 132870 (2023). https://doi.org/10.1016/j.snb.2022.132870
15. J.S. Chen, E. Ma, L.B. Harrington, M. Da Costa, X. Tian, J.M. Palefsky et al., CRISPR-Cas12a target binding unleashes indiscriminate single-stranded DNase activity. Science **360**(6387), 436–439 (2018). https://doi.org/10.1126/science.aar6245
16. B. Zetsche, J.S. Gootenberg, O.O. Abudayyeh, I.M. Slaymaker, K.S. Makarova, P. Essletzbichler et al., Cpf1 is a single RNA-guided endonuclease of a class 2 CRISPR-Cas system. Cell **163**(3), 759–771 (2015). https://doi.org/10.1016/j.cell.2015.09.038
17. D.P. Bartel, MicroRNAs: genomics, biogenesis, mechanism, and function. Cell **116**(2), 281–297 (2004). https://doi.org/10.1016/s0092-8674(04)00045-5
18. S. Xu, Y. Wang, Y. Yao, L. Chen, J. Xu, B. Qiu et al., Toehold-mediated strand displacement coupled with single nanoparticle dark-field microscopy imaging for ultrasensitive biosensing. Nanoscale **14**(9), 3496–3503 (2022). https://doi.org/10.1039/d1nr08030j
19. D.L. Chen, Y.X. Lu, J.X. Zhang, X.L. Wei, F. Wang, Z.L. Zeng et al., Long non-coding RNA UICLM promotes colorectal cancer liver metastasis by acting as a ceRNA for microRNA-215 to regulate ZEB2 expression. Theranostics. **7**(19), 4836–4849 (2017). https://doi.org/10.7150/thno.20942
20. R. Liu, S. Zhang, T.T. Zheng, Y.R. Chen, J.T. Wu, Z.S. Wu, Intracellular nonenzymatic in situ growth of three-dimensional DNA nanostructures for imaging specific biomolecules in living cells. ACS Nano **14**(8), 9572–9584 (2020). https://doi.org/10.1021/acsnano.9b09995
21. F. Yang, H. Lu, X. Meng, H. Dong, X. Zhang, Shedding light on DNA-based nanoprobes for live-cell MicroRNA imaging. Small **18**(10), e2106281 (2022). https://doi.org/10.1002/smll.202106281
22. C.M. Croce, G.A. Calin, miRNAs, cancer, and stem cell division. Cell **122**(1), 6–7 (2005). https://doi.org/10.1016/j.cell.2005.06.036
23. W. Fu-Ting, L. Hu, H. Yang-Yang, Y. Yu, H. Ke-Jing, L. Shu-Peng et al., Dual microRNAs-driven enzyme biofuel cells: visualization biosensing system with capacitor assistance output signal amplification. Sens. Actuators: B Chem. **365**, 131970 (2022). https://doi.org/10.1016/j.snb.2022.131970
24. Y. Du, L. Wang, H. Wu, Y. Zhang, K. Wang, D. Wu, MicroRNA-141 inhibits migration of gastric cancer by targeting zinc finger E-box-binding homeobox 2. Mol. Med. Rep. **12**(3), 3416–3422 (2015). https://doi.org/10.3892/mmr.2015.3789
25. X. Li, L. Liao, B. Jiang, W. Zhou, R. Yuan, Y. Xiang, Highly sensitive and label-free detection of DILI microRNA biomarker via target recycling and primer exchange reaction amplifications. Anal. Chim. Acta **1197**, 339521 (2022). https://doi.org/10.1016/j.aca.2022.339521
26. M. Hu, M. Xia, X. Chen, Z. Lin, Y. Xu, Y. Ma et al., MicroRNA-141 regulates Smad interacting protein 1 (SIP1) and inhibits migration and invasion of colorectal cancer cells. Dig. Dis. Sci. **55**(8), 2365–2372 (2010). https://doi.org/10.1007/s10620-009-1008-9
27. J. Shi, W.Z. Xie, L.R. Wang, Y.L. Song, Y. Lin, Y. Wu et al., All-carbon sandwich-type self-powered biosensor for ultrasensitive detection of femtomolar miRNA-141. Anal. Chim. Acta **1236**, 340589 (2022). https://doi.org/10.1016/j.aca.2022.340589
28. L. Lin, H. Liang, Y. Wang, X. Yin, Y. Hu, J. Huang et al., microRNA-141 inhibits cell proliferation and invasion and promotes apoptosis by targeting hepatocyte nuclear factor-3β in hepatocellular carcinoma cells. BMC Cancer **14**, 879 (2014). https://doi.org/10.1186/1471-2407-14-879
29. M. Lv, Y. Xu, R. Tang, J. Ren, S. Shen, Y. Chen et al., miR141-CXCL1-CXCR2 signaling-induced Treg recruitment regulates metastases and survival of non-small cell lung cancer. Mol. Cancer Ther. **13**(12), 3152–3162 (2014). https://doi.org/10.1158/1535-7163.Mct-14-0448
30. A. Khodadoust, N. Nasirizadeh, S.M. Seyfati, R.A. Taheri, M. Ghanei, H. Bagheri, High-performance strategy for the construction of electrochemical biosensor for simultaneous detection of miRNA-141 and miRNA-21 as lung cancer biomarkers. Talanta **252**, 123863 (2023). https://doi.org/10.1016/j.talanta.2022.123863
31. X. Liu, Q. Wang, Z. Diao, D. Huo, C. Hou, Label-free fluorescent biosensor based on AuNPs etching releasing signal for miRNA-155 detection. Talanta **278**, 126481 (2024). https://doi.org/10.1016/j.talanta.2024.126481
32. Q. Liu, M. Liu, Y. Jin, B. Li, Rapid and enzyme-free signal amplification for fluorescent detection of microRNA via localized catalytic hairpin assembly on gold nanoparticles. Talanta **242**, 123142 (2022). https://doi.org/10.1016/j.talanta.2021.123142
33. X. Zhang, X. Wei, J. Qi, J. Shen, J. Xu, G. Gong et al., Simultaneous detection of bladder cancer exosomal micrornas based on inorganic nanoflare and DNAzyme walker. Anal. Chem. **94**(11), 4787–4793 (2022). https://doi.org/10.1021/acs.analchem.1c05588
34. Y. Zhou, S. Yu, J. Shang, Y. Chen, Q. Wang, X. Liu et al., Construction of an exonuclease III-propelled integrated DNAzyme amplifier for highly efficient microRNA detection and intracellular imaging with ultralow background. Anal. Chem. **92**(22), 15069–15078 (2020). https://doi.org/10.1021/acs.analchem.0c03073
35. H. Wang, D. Wang, Y. Xu, Exonuclease-iii -propelled DNAzyme cascade for sensitive and reliable cervical cancer related miRNA analysis. Analy. Biochem. **691**, 115547 (2024). https://doi.org/10.1016/j.ab.2024.115547
36. Z. Xu, L. Yang, L.Q. Sun, Y. Cao, Use of DNAzymes for cancer research and therapy. Chin. Sci. Bull. **57**(26), 3404–3408 (2012). https://doi.org/10.1007/s11434-012-5380-z
37. J. Yan, M. Ran, X. Shen, H. Zhang, Therapeutic DNAzymes: from structure design to clinical applications. Adv. Mater. (Deerfield Beach, Fla) **35**(30), e2300374 (2023). https://doi.org/10.1002/adma.202300374
38. Z. Mao, R. Chen, X. Wang, Z. Zhou, Y. Peng, S. Li et al., CRISPR/Cas12a-based technology: a powerful tool for biosensing in food safety. Trends Food Sci. Technol. **122**, 211–222 (2022). https://doi.org/10.1016/j.tifs.2022.02.030
39. Y. Chen, X. Wang, J. Zhang, Q. Jiang, B. Qiao, B. He et al., Split crRNA with CRISPR-Cas12a enabling highly sensitive and multiplexed detection of RNA and DNA. Nat. Commun. **15**(1), 8342 (2024). https://doi.org/10.1038/s41467-024-52691-x

40. P.S. Mitchell, R.K. Parkin, E.M. Kroh, B.R. Fritz, S.K. Wyman, E.L. Pogosova-Agadjanyan et al., Circulating microRNAs as stable blood-based markers for cancer detection. Proc. Natl. Acad. Sci. U.S.A. **105**(30), 10513–10518 (2008). https://doi.org/10.1073/pnas.0804549105
41. Y.Q. Liu, M. Zhang, B.C. Yin, B.C. Ye, Attomolar ultrasensitive microRNA detection by DNA-scaffolded silver-nanocluster probe based on isothermal amplification. Anal. Chem. **84**(12), 5165–5169 (2012). https://doi.org/10.1021/ac300483f
42. Z. Xu, L. Liao, Y. Chai, H. Wang, R. Yuan, Ultrasensitive electrochemiluminescence biosensor for MicroRNA detection by 3D DNA walking machine based target conversion and distance-controllable signal quenching and enhancing. Anal. Chem. **89**(16), 8282–8287 (2017). https://doi.org/10.1021/acs.analchem.7b01409

Springer Nature or its licensor (e.g. a society or other partner) holds exclusive rights to this article under a publishing agreement with the author(s) or other rightsholder(s); author self-archiving of the accepted manuscript version of this article is solely governed by the terms of such publishing agreement and applicable law.